



# Transmuted lower record type inverse rayleigh distribution: estimation, characterizations and applications

Caner Tanış<sup>1</sup>

Received: 23 October 2021 / Revised: 11 April 2022 / Accepted: 25 April 2022 /

Published online: 23 May 2022

© Università degli Studi di Napoli "Federico II" 2022

## Abstract

This study introduces a new lifetime distribution called the transmuted lower record type inverse Rayleigh which extends the inverse Rayleigh distribution and has the potential to model the recovery times of Covid-19 patients. The new distribution is obtained using the distributions of the first two lower record statistics of the inverse Rayleigh distribution. We discuss some statistical inferences and mathematical properties of the suggested distribution. We examine some characteristics of the proposed distribution such as density shape, hazard function, moments, moment generating function, incomplete moments, Rényi entropy, order statistics, stochastic ordering. We consider five estimation methods such as maximum likelihood, least squares, weighted least squares, Anderson-Darling, Cramér-von Mises for the point estimation of the proposed distribution. Then, a comprehensive Monte Carlo simulation study is carried out to assess the risk behavior of the examined estimators. We provide two real data applications to illustrate the fitting ability of the proposed model, and compare its fit with competitor ones. Unlike many previously proposed distributions, the introduced distribution in this paper has modeled the recovery times of Covid-19 patients.

**Keywords** Inverse Rayleigh distribution · Lower records · Point estimation · Covid-19

## 1 Introduction

In recent years, many lifetime distributions have been proposed in the literature. The lifetime distributions are useful in various fields such as agriculture, actuarial, biology, engineering, and medical sciences. These distributions have emerged via different methods. One of these methods is the quadratic rank transmutation map (QTRM), which is based on order statistics. The QRTM was proposed by [1] to generate a

---

✉ Caner Tanış  
canertanis@karatekin.edu.tr

<sup>1</sup> Department of Statistics, Science Faculty, Çankırı Karatekin University, Çankırı, Turkey

**Table 1** Some transmuted distributions in the literature

Baseline distribution	Author(s)
Weibull	[2]
Lindley	[3]
Rayleigh	[4]
Inverse Rayleigh	[5]
Exponentiated Inverse Rayleigh	[6]
Generalized Modified Weibull	[7]
Complementary Exponential Power	[8]
Exponential Power	[9]

new distribution using the distributions of the first two order statistics. QRTM is summarized as follows:

Let  $X_{1:n}, X_{2:n}$  be the order statistics from a population with cumulative distribution function (cdf)  $G(\cdot)$  and probability density function (pdf)  $g(\cdot)$  and  $n$  denotes sample sizes.

Let us define random variable  $Y$  by

$$\begin{aligned} Y &\stackrel{d}{=} X_{1:2}, \text{ with probability } \pi \\ Y &\stackrel{d}{=} X_{2:2}, \text{ with probability } 1 - \pi, \end{aligned}$$

where  $\pi \in (0, 1)$ . The, the cdf of  $Y$  is given by

$$\begin{aligned} F_Y(x) &= \pi P(X_{1:2} \leq x) + (1 - \pi) P(X_{2:2} \leq x) \\ &= \pi \left(1 - (1 - G(x))^2\right) + (1 - \pi) G^2(x) \\ &= 2\pi G(x) + (1 - 2\pi) G^2(x). \end{aligned} \quad (1)$$

Substituting  $\pi = \frac{1+\lambda}{2}$  in (1) the cdf and corresponding pdf are obtained by

$$F(x) = (1 + \lambda) G(x) - \lambda [G(x)]^2 \quad (2)$$

and

$$f(x) = (1 + \lambda) g(x) - 2\lambda G(x) g(x), \quad (3)$$

respectively, where  $\lambda \in [-1, 1]$ . The generated distributions by using QRTM are called transmuted distributions. In last decade, many transmuted distributions are suggested in the literature, and some transmuted distributions are given in Table 1.

In addition to Table 1, [10] introduced a generalized family of transmuted distribution. [11] proposed a new method called cubic rank map (CRTM) with the motivation of the QRTM. The CRTM is summarized as follows:

Let  $X_{1:n}, X_{2:n}$  and  $X_{3:n}$  be the order statistics from a population with cdf  $G(x)$  and pdf  $g(x)$ .

Let us define a random variable  $Y$  by

$$\begin{aligned}
 Y &\stackrel{d}{=} X_{1:3}, \text{ with probability } \pi_1 \\
 Y &\stackrel{d}{=} X_{2:3}, \text{ with probability } \pi_2 \\
 Y &\stackrel{d}{=} X_{3:3}, \text{ with probability } \pi_3,
 \end{aligned}$$

where  $\pi_1 + \pi_2 + \pi_3 = 1$ . Thus, the cdf of  $Y$  is given by

$$\begin{aligned}
 F_Y(x) &= \pi_1 P(X_{1:3} \leq x) + \pi_2 P(X_{2:3} \leq x) + \pi_3 P(X_{3:3} \leq x) \\
 &= \pi_1 \left[ 1 - (1 - G(x))^3 \right] + 6\pi_2 \int_0^x G(t)(1 - G(t))g(t) dt + \pi_3 G^3(x) \\
 &= 3\pi_1 G(x) + (3\pi_2 - 3\pi_1) G^2(x) + (1 - 3\pi_2) G^3(x)
 \end{aligned} \tag{4}$$

Substituting  $3\pi_1 = \lambda_1, 3\pi_2 = \lambda_2$  in (4), the cdf and pdf of cubic rank transmuted distribution are given by

$$F_Y(x) = \lambda_1 G(x) + (\lambda_2 - \lambda_1) G^2(x) + (1 - \lambda_2) G^3(x), \tag{5}$$

and

$$f_Y(x) = g(x) \lambda [1 + 2(\lambda_2 - \lambda_1) G(x)] + 3(1 - \lambda_2) g(x) G^2(x), \tag{6}$$

respectively, where  $\lambda_1 \in [0, 1], \lambda_2 \in [-1, 1]$ . The generated distributions via the CRTM are called cubic rank transmuted distributions. In the literature, some cubic rank transmuted distributions are listed in Table 2.

[17] provided a generalization of cubic rank transmuted distributions. [18] suggested a new method based on the distributions of first two upper records called transmuted upper record type map (TRTM) to produce distributions. They described the TRTM in [18] as follows:

**Table 2** Some cubic transmuted distributions in the literature

Baseline distribution	Authors
Weibull	[11]
Log-logistic	[11]
Kumaraswamy	[12]
Inverse Weibull	[13]
Modified Burr III	[14]
Modified Burr III Pareto	[15]
Lindley	[16]

Let  $X_{U(1)}$  and  $X_{U(2)}$  be upper records from a population with cdf  $G(\cdot)$  and pdf  $g(\cdot)$ .

Let us describe a random variable  $Y$  by

$$\begin{aligned} Y &\stackrel{d}{=} X_{U(1)}, \text{ with probability } \pi_1 \\ Y &\stackrel{d}{=} X_{U(2)}, \text{ with probability } \pi_2, \end{aligned}$$

where  $\pi_1 + \pi_2 = 1$ . In this case, the cdf of  $Y$  is given by

$$\begin{aligned} F_Y(x) &= \pi_1 P(X_{U(1)} \leq x) + \pi_2 P(X_{U(2)} \leq x) \\ &= \pi_1 G(x) + \pi_2 \left[ 1 - \sum_{R=0}^1 \frac{(-\log(1-G(x)))^R}{R!} (1-G(x)) \right] \\ &= G(x) + p(1-G(x)) \times \log(1-G(x)), \end{aligned} \quad (7)$$

where  $\pi_2 = p$ ,  $\pi_1 = 1 - p$ ,  $p \in (0, 1)$ . Then, the corresponding pdf of  $Y$  is

$$f_Y(x) = g(x) [1 + p(-\log(1-G(x)) - 1)] \quad (8)$$

[19] discussed some mathematical properties and estimation methods of a special case based on Weibull distribution of the family of record-based transmuted distributions. Balakrishnan and He [18] also provided the record-based family of distributions which is a mixture based on the distributions of the first two lower record values. This family of distributions is constructed by

Let  $X_{L(1)}$  and  $X_{L(2)}$  be the lower record values from a population with the cdf  $G(x)$ .

Let us define a new random variable based on these records:

$$Y = \begin{cases} X_{L(1)}, & U > p \\ X_{L(2)}, & U < p, \end{cases}$$

where  $U$  is standard uniform random variable and  $p \in (0, 1)$ . The cdf of  $Y$  is obtained by

$$\begin{aligned} F(x) &= (1-p) P(X_{L(1)} \leq x) + p P(X_{L(2)} \leq x) \\ &= (1-p) G(x) + p [G(x) (1 - \log(G(x)))] \\ &= G(x) [1 - p \log(G(x))]. \end{aligned} \quad (9)$$

Balakrishnan and He [18] noticed that the distribution with cdf (9) is called dual record-transmuted distribution. In this paper, we call this family of distributions as the family of transmuted lower record type (TLRT) distributions. The corresponding pdf and hazard function(hf) of TLRT distribution are given by

$$f(x) = g(x) [1 - p(1 + \log(G(x)))] \quad (10)$$

and

$$h(x) = \frac{g(x) [1 - p(1 + \log(G(x)))]}{1 - G(x) [1 - p \log(G(x))]}, \tag{11}$$

respectively. [20] proposed the first sub-model of the family of TLRT distributions called transmuted lower record type Fréchet distribution.

Transmuted lower record type method (TLRTM) defined in (14) and (15) allows to be proposed a new distribution via the mixture of the distributions of the lower record values. For instance, let consider an Olympic athlete who broke more than one record in the Olympics and assume that this athlete achieve first and second records with certain probabilities. The new mixed distribution produced with TLRTM can be associated with this situation in real life. The motivation of this paper is to generate a new special case based on inverse Rayleigh by using TLRTM. We aim to provide a new flexible version of inverse Rayleigh distribution for modelling the data in medical sciences and other fields. Unlike previously proposed distributions, an important advantage of the suggested distribution is that it models the recovery times of COVID-19 patients. The study is organized as follows: In Sect. 2, some distributional properties of the suggested distribution are examined such as density shapes, moments, incomplete moments, moment generating function, Rényi entropy, stochastic ordering, and order statistics. In Sect. 3, we obtain five estimators of the parameters of the introduced distribution such as maximum likelihood estimators (MLEs), least squares estimators (LSEs), weighted least squares estimators (WLSEs), Anderson-Darling estimators (ADEs), and Cramér-von Mises estimators (CvMEs). A comprehensive simulation study is considered to compare the performances of the examined estimators according to mean squared errors (MSEs) and biases in Sect. 4. Section 5 presents two real data applications regarding the recovery times of COVID-19 patients to illustrate the applicability of the introduced distribution, and we show that it has the potential for modelling datasets in medical sciences. Finally, conclusions are given in Sect. 6.

## 2 Transmuted lower record type inverse rayleigh distribution and distributional properties

In this section, we introduce a new lifetime distribution called transmuted lower record type inverse Rayleigh (TLRTIR) by using the TLRTM.

Let  $X$  be a random variable from inverse Rayleigh distribution. The cdf and pdf of  $X$  are given as follows:

$$G(x) = \exp\left(-\frac{\alpha}{x^2}\right), \tag{12}$$

and

$$g(x) = \frac{2\alpha}{x^3} \exp\left(-\frac{\alpha}{x^2}\right) \tag{13}$$

respectively, where,  $\alpha > 0$  and  $x > 0$ . Substituting the cdf (12) and pdf (13) into (9) and (10), then the cdf and pdf of TRTLIR distribution are

$$F(x; \alpha, p) = \exp\left(-\frac{\alpha}{x^2}\right) \left(1 + \frac{p\alpha}{x^2}\right) \tag{14}$$

and

$$f(x; \alpha, p) = \frac{2\alpha}{x^3} \exp\left(-\frac{\alpha}{x^2}\right) \left[1 - p \left(1 - \frac{\alpha}{x^2}\right)\right], \tag{15}$$

respectively, where  $\alpha > 0$ ,  $p \in (0, 1)$  and  $x > 0$ . The distribution with cdf (14) is called “transmuted lower record type inverse Rayleigh (TLRTIR( $\alpha, p$ ))”distribution.

### 2.1 Density shape

In this section, we examine some possible density shapes of TLRTIR ( $\alpha, p$ ) distribution.

**Theorem 2.1** *Let  $X$  be a random variable from TLRTIR ( $\alpha, p$ ) distribution. The pdf of TLRTIR ( $\alpha, p$ ) distribution is unimodal for  $p > \frac{12}{17}$ .*

**Proof** Let  $T_1(x) = \frac{d}{dx} \log \{f_{TLRTIR}(x)\}$  and  $T_2(x) = \frac{d^2}{dx^2} \log \{f_{TLRTIR}(x)\}$  are given by

$$T_1(x) = \frac{(3 - 3p)x^4 + (7p\alpha - 2\alpha)x^2 - 2p\alpha^2}{x^3 \{(p - 1)x^2 - p\alpha\}} \tag{16}$$

and

$$T_2(x) = \frac{\varpi(x, \alpha, p) + 17\alpha^2 p \left(p - \frac{12}{17}\right)x^2 - 6p^2\alpha^3}{\{(p - 1)x^2 - p\alpha\}x^4} \tag{17}$$

where,

$$\varpi(x, \alpha, p) = 3(p - 1)^2 x^6 - 18\alpha(p - 1)\left(p - \frac{1}{3}\right)x^4.$$

We observe that  $T_2(x) < 0$  for  $p > \frac{12}{17}$ , and the density of TLRTIR ( $\alpha, p$ ) distribution has log-concavity property. The proof is completed. □

Thus, it can be concluded that the density of the TLRTIR ( $\alpha, p$ ) distribution is unimodal for  $p > \frac{12}{17}$  according to Theorem 1. The hf of the TLRTIR( $\alpha, p$ ) distribution is given by

$$h(x; \alpha, p) = \frac{\frac{2\alpha}{x^3} \exp\left(-\frac{\alpha}{x^2}\right) \left[1 - p \left(1 - \frac{\alpha}{x^2}\right)\right]}{1 - \exp\left(-\frac{\alpha}{x^2}\right) \left(1 + \frac{p\alpha}{x^2}\right)} \tag{18}$$

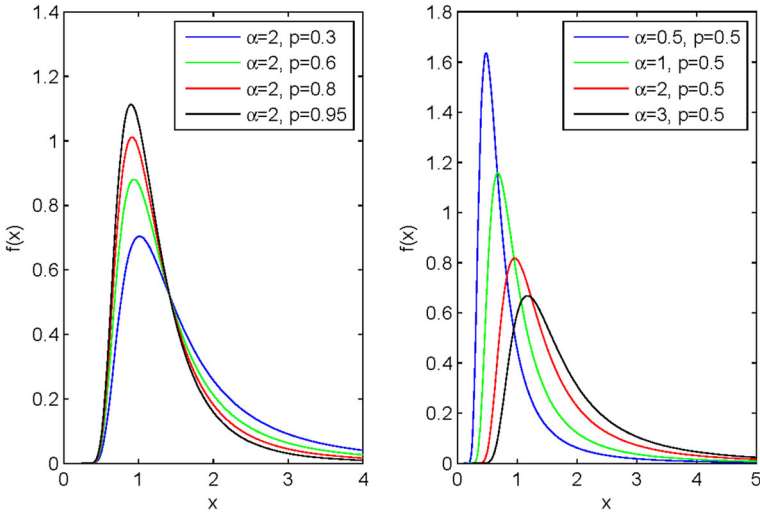


Fig. 1 The pdf plots for TLRTIR( $\alpha, p$ ) distribution

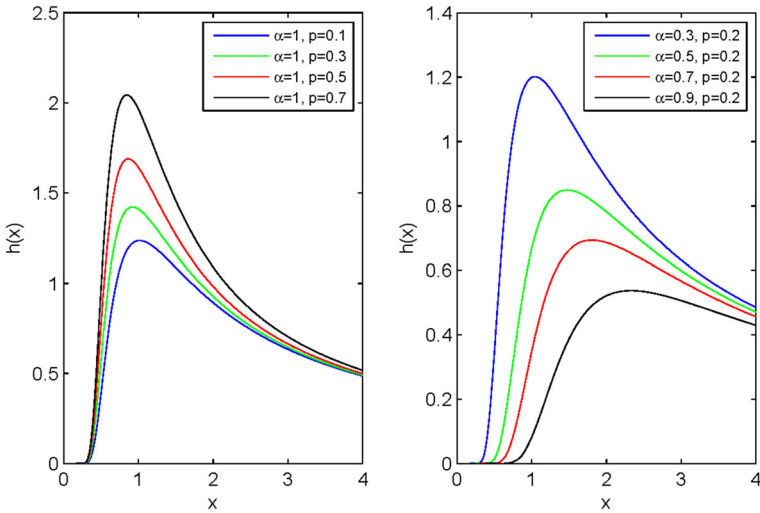


Fig. 2 The hf plots of TLRTIR ( $\alpha, p$ ) distribution

Figures 1 and 2 illustrate the possible pdf and hf shapes of the TLRTIR ( $\alpha, p$ ) distribution for the selected parameter values respectively.

From Figure 2, it is seen that the TLRTIR ( $\alpha, p$ ) distribution has upside bathtub shaped hf for selected parameters.

## 2.2 Moments

The  $r^{\text{th}}$  raw moment of TLRTIR( $\alpha, p$ ) distribution for  $r \in \mathbb{N}_+$  is given by

$$E(X^r) = (1-p)\alpha^{r/2}\Gamma\left(\frac{2-r}{2}\right) + p\alpha^{(r+1)/2}\Gamma\left(\frac{3-r}{2}\right), \quad (19)$$

where  $\Gamma(\cdot)$  is a gamma function.

## 2.3 Moment generating function

The moment generating function of TLRTIR ( $\alpha, p$ ) distribution is given by

$$\begin{aligned} M(t) &= (1-p) \sum_{r=0}^{\infty} \frac{t^r}{r!} \alpha^{r/2} \Gamma\left(\frac{2-r}{2}\right) \\ &\quad + p \sum_{r=0}^{\infty} \frac{t^r}{r!} \alpha^{(r+1)/2} \Gamma\left(\frac{3-r}{2}\right). \end{aligned} \quad (20)$$

## 2.4 Incomplete moments

The incomplete moments of TLRTIR distribution is given by

$$\begin{aligned} m_r(y) &= (1-p)\alpha^{r/2}\Gamma\left(\frac{2-r}{2}, \frac{\alpha}{t^2}\right) \\ &\quad + p\alpha^{(r+1)/2}\Gamma\left(\frac{3-r}{2}, \frac{\alpha}{t^2}\right), \end{aligned} \quad (21)$$

where  $\Gamma(a, x)$  is incomplete gamma function defined by

$$\Gamma(a, x) = \int_x^{\infty} t^{a-1} e^{-t} dt.$$

## 2.5 Rényi entropy

The Rényi entropy is proposed by Rényi [21]. The Rényi entropy is a measure of uncertainty, and it is defined by

$$I_R(\rho) = \frac{1}{1-\rho} \log \left\{ \int f(x)^\rho dx \right\}, \quad (22)$$

where  $\rho > 0$  and  $\rho \neq 1$ .



**Theorem 2.2** *The Rényi entropy for TLRTIR( $\alpha, p$ ) distribution is*

$$I_R(\rho) = \frac{1}{1-\rho} \left[ \log \left\{ \varphi(\rho) \sum_{j=0}^{\rho} \frac{p^{\rho-j} (1-p)^j \Gamma(10\rho - 4j - 2)}{\Gamma(\rho - j + 1) \Gamma(j + 1)} \right\} \right], \tag{23}$$

where,  $\varphi(\rho) = \frac{2^{\rho-1} \alpha^{(\rho-1)/2} \Gamma(\rho+1)}{\rho^{(3\rho+1)/2}}$ ,  $\rho \neq 1$  and  $\rho \in \mathbb{Z}$ .

**Proof** The Rényi entropy of TLRTIR( $\alpha, p$ ) distribution can be written using (22) as follows:

$$I_R(\rho) = \frac{1}{1-\rho} \log \left\{ \int \left( \frac{2\alpha}{x^3} \right)^{\rho} \exp\left(-\frac{\rho\alpha}{x^2}\right) \left[ 1 - p \left( 1 - \frac{\alpha}{x^2} \right) \right]^{\rho} dx \right\} \tag{24}$$

Using  $u = \frac{\rho\alpha}{x^2}$  transformation in (24), the integral is obtained by

$$\int_0^{\infty} f(x)^{\rho} dx = \int_0^{\infty} \frac{(2\alpha)^{\rho-1} \exp(-u) [1 - p + pu]^{\rho}}{\rho \left( \frac{\rho\alpha}{u} \right)^{3(\rho-1)/2}} du, \tag{25}$$

Then, using power series expansion of  $(1 - p + pu)^{\rho} = \sum_{j=0}^{\rho} \binom{\rho}{j} (1-p)^j p^{\rho-j} u^{\rho-j}$  defined in [22], Eq. (25) is obtained as follows:

$$\begin{aligned} \int_0^{\infty} f(x)^{\rho} dx &= \frac{2^{\rho-1} \alpha^{(\rho-1)/2}}{\rho^{(3\rho+1)/2}} \sum_{j=0}^{\rho} \frac{p^{\rho-j} (1-p)^j \Gamma(\rho+1)}{\Gamma(\rho-j+1) \Gamma(j+1)} \int_0^{\infty} u^{(5\rho-2j-3)/2} \exp(-u) du \\ &= \frac{2^{\rho-1} \alpha^{(\rho-1)/2} \Gamma(\rho+1)}{\rho^{(3\rho+1)/2}} \sum_{j=0}^{\rho} \frac{p^{\rho-j} (1-p)^j \Gamma(10\rho - 4j - 2)}{\Gamma(\rho-j+1) \Gamma(j+1)} \end{aligned} \tag{26}$$

By substituting (26) into (24), Thus, the Rényi entropy in (23) and the proof is completed. □

**2.6 Order statistics**

Let  $X_{1:n}, X_{2:n}, \dots, X_{n:n}$  be the order statistics from a population with cdf (14) and pdf (15). The pdf of  $j^{th}$  order statistics,  $X_{j:n}$ ,  $j = 1, \dots, n$  is given by

$$\begin{aligned} f_{X_{j:n}}(x) &= \frac{n!}{(j-1)!(n-j)!} f(x) F^{j-1}(x) [1 - F(x)]^{n-j} \\ &= \frac{n!}{(j-1)!(n-j)!} \frac{2\alpha}{x^3} \exp\left(-\frac{\alpha}{x^2}\right) \left[ 1 - p \left( 1 - \frac{\alpha}{x^2} \right) \right] \\ &\quad \times \sum_{i=0}^{n-j} (-1)^j \binom{n-j}{i} \exp\left(-\frac{(i+j-1)\alpha}{x^2}\right) \left[ 1 + p \frac{\alpha}{x^2} \right]^{i+j-1}. \end{aligned} \tag{27}$$

## 2.7 Stochastic ordering

Stochastic and the other ordering are important means for evaluating the comparative properties for a positive continuous random variable [20]. The following theorem shows that the TLRTIR random variables can be ordered with respect to the likelihood ratio.

**Theorem 2.3** *Let  $X \sim \text{TLRTIR}(\alpha, p_1)$  and  $Y \sim \text{TLRTIR}(\alpha, p_2)$ . If  $p_1 > p_2$  then  $X$  is smaller than  $Y$  in the likelihood ratio order, i.e., the ratio function of the corresponding pdfs is decreasing in  $x$ .*

**Proof** For any  $x > 0$ , the ratio of the densities is given by

$$g(x) = \frac{1 - p_1 \left(1 - \frac{\alpha}{x^2}\right)}{1 - p_2 \left(1 - \frac{\alpha}{x^2}\right)}.$$

Consider the derivative of  $\log(g(x))$  in  $x$

$$\frac{d \log(g(x))}{dx} = \frac{-2\alpha x (p_1 - p_2)}{m(x, \alpha, p_1, p_2)}$$

where,

$$m(x, \alpha, p_1, p_2) = \left((p_1 - 1)x^2 - p_1\alpha\right) \times \left((p_2 - 1)x^2 - p_2\alpha\right)$$

It is seen that  $\frac{d \log(g(x))}{dx} < 0$  for  $p_1 > p_2$  and hence proof is completed.  $\square$

**Corollary 2.4** *It follows from [23] that  $X$  is also smaller than  $Y$  in the hazard ratio, and stochastic orders under the conditions given in Theorem 2.3.*

## 2.8 Random numbers generation

In order to generate the data from TLRTIR  $(\alpha, p_1)$  distribution, an acceptance-rejection (AR) sampling method is given in the following algorithm. In this algorithm, the Weibull distribution is chosen as a proposal distribution. The AR algorithm is given as follows:

### Algorithm 1.

**A1.** Generate data on random variable  $Y$  from Weibull distribution with pdf  $g$  given as follow:

$$g(\alpha, \beta) = \frac{\alpha}{\beta} \left(\frac{y}{\beta}\right)^{\alpha-1} \exp\left(-\left(\frac{y}{\beta}\right)^\alpha\right).$$

**A2.** Generate  $U$  from standard uniform distribution(independent of  $Y$ ).

**A3.** If

$$U < \frac{f(Y; \alpha, p)}{k \times g(Y; \alpha, \beta)}$$

then set  $X = Y$  (“accept”); otherwise go back to A1 (“reject”), where pdf  $f$  is given as in (15) and

$$k = \max_{z \in \mathbb{R}_+} \frac{f(z; \alpha, p)}{g(z; \alpha, \beta)}.$$

The output of this algorithm suggests a random data on  $X$  from TLRTIR( $\alpha, p$ ). It is noticed that the Algorithm 1 is used for all simulations in the paper.

### 3 Point estimation

In this section, we examine five estimators for point estimation of the TLRTIR ( $\alpha, p$ ) distributions such as MLEs, LSEs, WLSEs, ADEs, and CVMEs.

#### 3.1 Maximum likelihood estimation

Let  $X_1, X_2, \dots, X_n$  be a random sample from TLRTIR( $\alpha, p$ ) distribution. The log-likelihood function is given by;

$$\ell(\alpha, p|\mathbf{x}) = n \log 2\alpha - \sum_{i=1}^n \frac{\alpha}{x_i^2} - 3 \sum_{i=1}^n \log x_i + \sum_{i=1}^n \log \left( 1 - p \left( 1 - \frac{\alpha}{x_i^2} \right) \right), \tag{28}$$

where  $\mathbf{x} = (x_1, x_2, \dots, x_n)$ . The MLEs,  $\hat{\alpha}_{MLE}$  and  $\hat{p}_{MLE}$ , of  $\alpha$  and  $p$  are obtained by simultaneously solving the following log-likelihood equations.

$$\frac{\partial \ell(\alpha, p|\mathbf{x})}{\partial \alpha} = \frac{n}{\alpha} - \sum_{i=1}^n \frac{1}{x_i^2} + \sum_{i=1}^n \frac{p}{x_i^2 \left( 1 - p \left( 1 - \frac{\alpha}{x_i^2} \right) \right)} = 0, \tag{29}$$

$$\frac{\partial \ell(\alpha, p|\mathbf{x})}{\partial p} = \sum_{i=1}^n \frac{\frac{\alpha}{x_i^2} - 1}{1 - p \left( 1 - \frac{\alpha}{x_i^2} \right)} = 0. \tag{30}$$

The log-likelihood equations (29)-(30) can be solved using numerical methods such as Nelder-Mead, Broyden-Fletcher-Goldfarb-Shanno (BFGS). This algorithm is firstly studied by Fletcher [24]. These methods can be easily employed by optim function in R. The following results regarding to singularity of  $\hat{\alpha}_{MLE}$  of the parameter  $\alpha$ .

**Theorem 3.1** *Let us assume that the parameter  $p$  is known. There exists a unique MLE of the parameter  $\alpha$  for  $p \in (0, 1)$ .*

**Proof** We obtained the second derivative of the log-likelihood function (3.1) according to the parameter  $\alpha$  as follows:

$$\frac{\partial^2 \ell(\alpha, p|\mathbf{x})}{\partial \alpha^2} = -\frac{n}{\alpha^2} - \sum_{i=1}^n \frac{p^2}{x_i^4 \left\{ 1 - p \left( 1 - \frac{\alpha}{x_i^2} \right) \right\}^2}$$

Since  $p \in (0, 1)$ , it follows that  $\frac{\partial^2 \ell(\alpha, p|\mathbf{x})}{\partial \alpha^2} < 0$ , which means that  $\frac{\partial \ell(\alpha, p|\mathbf{x})}{\partial \alpha}$  is a decreasing function. Further, it is clearly seen that  $\lim_{\alpha \rightarrow 0} \frac{\partial \ell(\alpha, p|\mathbf{x})}{\partial \alpha} = \infty$  and  $\lim_{\alpha \rightarrow \infty} \frac{\partial \ell(\alpha, p|\mathbf{x})}{\partial \alpha} = -\sum_{i=1}^n \frac{1}{x_i^2} < 0$ , which provides the uniqueness of  $\hat{\alpha}_{MLE}$ . Thus, the proof is completed.  $\square$

### 3.2 Ordinary least squares and weighted least squares estimation

Let  $X_1, X_2, \dots, X_n$  be a random sample from TLRTIR( $\alpha, p$ ) distribution, and  $x_{1:n} < x_{2:n} < \dots < x_{n:n}$  denote the corresponding observed order statistics. The LSEs,  $\hat{\alpha}_{LSE}$  and  $\hat{p}_{LSE}$ , of  $\alpha$  and  $p$  are obtained by minimizing

$$Z(\alpha, p) = \sum_{i=1}^n \left[ F(X_{i:n}, \alpha, p) - \frac{i}{n+1} \right]^2, \quad (31)$$

with respect to  $\alpha$  and  $p$  parameters. The weighted least squares estimators (WLSEs),  $\hat{\alpha}_{WLSE}$  and  $\hat{p}_{WLSE}$ , of  $\alpha$  and  $p$  are derived by minimizing following equation with respect to  $\alpha$  and  $p$  parameters.

$$\varpi(\alpha, p) = \sum_{i=1}^n \frac{(n+1)^2 (n+2)}{i(n-i+1)} \times \left[ \left( F(X_{i:n}, \alpha, p) - \frac{i}{n+1} \right) \right]^2, \quad (32)$$

where cdf  $F(\cdot)$  is given as in (14)

### 3.3 Anderson-darling estimation

The ADEs,  $\hat{\alpha}_{ADE}$  and  $\hat{p}_{ADE}$  of  $\alpha$  and  $p$  are obtained by minimizing following equation with respect to  $\alpha$  and  $p$  parameters.

$$A(\alpha, p) = -n - \frac{1}{n} \sum_{i=1}^n (2i-1) (\log F(X_{i:n}, \alpha, p) + \log \bar{F}(X_{i:n}, \alpha, p)). \quad (33)$$

### 3.4 Cramér-von mises estimation

The CMEs  $\hat{\alpha}_{CME}$  and  $\hat{p}_{CME}$  of  $\alpha$  and  $p$  are derived by minimizing following equation with respect to  $\alpha$  and  $p$  parameters.

$$C(\alpha, p) = \frac{1}{12n} + \sum_{i=1}^n \left( F(X_{i:n}, \alpha, p) - \frac{2i-1}{2n} \right)^2. \quad (34)$$

## 4 Simulation study

In this subsection, we perform a Monte Carlo simulation study. In the simulation study, MSEs and biases of five estimators are calculated with 5000 repetitions for the sample sizes such as  $n=50, 100, 250, 500, 750$  and  $1000$ . Five parameter settings are considered as follows:  $(\alpha = 0.3, p = 0.3)$ ,  $(\alpha = 0.7, p = 0.9)$ ,  $(\alpha = 1, p = 0.5)$ ,  $(\alpha = 2, p = 0.7)$ ,  $(\alpha = 3, p = 0.9)$ . In all simulations, the samples are generated from TLRTIR  $(\alpha, p)$  distribution by using AR sampling given in Algorithm 1. The biases and MSEs of the estimators are given in Tables 3, 7.

According to Tables 3, 4, 5, 6 and 7, it is observed that as the sample sizes increase, the biases and MSEs of the all estimators decrease and approach to zero. For parameter  $p$ , the performances of MLEs are generally better than the other estimators in terms of MSEs and biases. On the other hand, it is seen that the best estimator is ADE in small sample sizes while MLE is the best estimator in large sample sizes according to MSE and bias for point estimation of parameter  $\alpha$ . As a result of the simulation study, we recommend the maximum likelihood method and Anderson-Darling method for point estimation of parameters of TLRTIR  $(\alpha, p)$  distribution.

## 5 Real data analysis

In this section, we perform two real data applications to illustrate the usefulness of TLRTIR  $(\alpha, p)$  distribution in modelling real-life data. In real data analysis, two datasets are fitted to TLRTIR  $(\alpha, p)$ , transmuted inverse Rayleigh (TIR  $(\alpha, \lambda)$ ) [5], inverse Rayleigh (IR  $(\alpha)$ ), transmuted Rayleigh (TR  $(\alpha, \lambda)$ ) [4], transmuted Weibull (TW  $(\alpha, \beta, \lambda)$ ) [2], Weibull  $(\alpha, \beta)$ , Rayleigh  $(\alpha)$ , transmuted record type Weibull (TRTW  $(\alpha, \beta, p)$ ) [18] distributions. The pdfs of fitted distributions are listed in Table 8.

In order to compare the fitted distribution, some selection statistics such as Akaike's information criterion (AIC), Bayesian information criterion (BIC), Anderson-Darling (A\*), Cramer von Mises (W\*), Kolmogorov-Smirnov (K-S) test statistics and its p-value are used.

**Table 3** Average bias and MSEs of the estimators for  $\alpha = 0.3$  and  $p = 0.3$ 

		Bias		MSE	
		$\hat{\alpha}$	$\hat{p}$	$\hat{\alpha}$	$\hat{p}$
MLE	50	0.049664	0.068824	0.00842	0.070459
	100	0.026747	0.019832	0.004448	0.050308
	250	0.010469	-0.01022	0.002162	0.030212
	500	0.005703	-0.01236	0.001215	0.018199
	750	0.004496	-0.01093	0.000895	0.013646
	1000	0.001791	-0.01702	0.000644	0.010161
	5000	0.000493	-0.0085	0.000109	0.001724
LSE	50	0.032189	0.002717	0.007961	0.075084
	100	0.018769	-0.0146	0.004617	0.055491
	250	0.005786	-0.03001	0.002624	0.037136
	500	0.00196	-0.0274	0.001597	0.023545
	750	-0.00069	-0.03167	0.001431	0.022892
	1000	-0.00173	-0.03103	0.001031	0.016086
	5000	$-9.3 \times 10^{-5}$	-0.01084	0.000184	0.002691
WLSE	50	0.03502	0.011656	0.008007	0.077188
	100	0.020739	-0.00689	0.004484	0.056185
	250	0.004852	-0.03444	0.002741	0.042562
	500	0.00226	-0.02651	0.001547	0.025085
	750	0.003175	-0.01606	0.001012	0.015469
	1000	0.000281	-0.02301	0.000802	0.012796
	5000	0.00032	-0.00919	0.000136	0.002097
ADE	50	0.034733	0.012024	0.007586	0.081607
	100	0.022988	0.002217	0.004177	0.05087
	250	0.008604	-0.01858	0.002225	0.032055
	500	0.001474	-0.02985	0.001608	0.026403
	750	0.002873	-0.01732	0.001022	0.015749
	1000	0.000202	-0.0233	0.000787	0.012533
	5000	0.000266	-0.00939	0.000134	0.00207
CvME	50	0.053395	0.067505	0.010383	0.082356
	100	0.029976	0.021029	0.00538	0.056922
	250	0.011018	-0.0125	0.002738	0.03632
	500	0.004874	-0.01745	0.001609	0.022777
	750	0.001504	-0.02395	0.001404	0.021858
	1000	-0.00014	-0.02552	0.001015	0.015504
	5000	0.000217	-0.00977	0.000183	0.002649

**Table 4** Average bias and MSEs of the estimators for  $\alpha = 0.7$  and  $p = 0.9$

		Bias		MSE	
		$\hat{\alpha}$	$\hat{p}$	$\hat{\alpha}$	$\hat{p}$
MLE	50	0.004532	-0.09673	0.008028	0.028921
	100	0.009934	-0.05253	0.003927	0.011603
	250	0.0089	-0.02491	0.001666	0.004334
	500	0.007633	-0.01442	0.000887	0.002213
	750	0.005716	-0.01163	0.00059	0.001528
	1000	0.00493	-0.00994	0.000441	0.00112
	5000	0.002069	-0.00454	$8.48 \times 10^{-5}$	0.000214
LSE	50	-0.01939	-0.13143	0.012882	0.060167
	100	-0.00121	-0.06824	0.005696	0.022617
	250	0.004767	-0.03116	0.002316	0.008213
	500	0.005102	-0.01828	0.001153	0.003794
	750	0.004289	-0.01403	0.000774	0.002592
	1000	0.003348	-0.01287	0.000581	0.001967
	5000	0.00186	-0.00482	0.000115	0.000373
WLSE	50	-0.01456	-0.1266	0.0114	0.057153
	100	0.001919	-0.06481	0.005205	0.022039
	250	0.006696	-0.02798	0.001842	0.005572
	500	0.006418	-0.01613	0.000949	0.002701
	750	0.00506	-0.01262	0.000639	0.001873
	1000	0.004202	-0.01122	0.000482	0.001416
	5000	0.001965	-0.00466	$9.43 \times 10^{-5}$	0.000269
ADE	50	-0.01059	-0.11797	0.00915	0.04163
	100	0.002661	-0.06243	0.004162	0.014911
	250	0.006094	-0.02905	0.001778	0.005381
	500	0.005952	-0.01697	0.000934	0.002684
	750	0.004719	-0.01322	0.00063	0.001865
	1000	0.003957	-0.01166	0.000477	0.001413
	5000	0.001905	-0.00476	$9.4 \times 10^{-5}$	0.00027
CvME	50	0.006198	-0.08132	0.012182	0.045509
	100	0.010539	-0.04516	0.005809	0.019822
	250	0.009388	-0.02182	0.002327	0.007206
	500	0.007335	-0.01378	0.00118	0.003635
	750	0.00577	-0.01104	0.000788	0.002511
	1000	0.004456	-0.01063	0.000589	0.00191
	5000	0.002079	-0.00438	0.000116	0.000368

**Table 5** Average bias and MSEs of the estimators for  $\alpha = 1$  and  $p = 0.5$ 

		Bias		MSE	
		$\hat{\alpha}$	$\hat{p}$	$\hat{\alpha}$	$\hat{p}$
MLE	50	0.07328	-0.0167	0.052078	0.066896
	100	0.047856	-0.01732	0.028987	0.041861
	250	0.026077	-0.0181	0.011296	0.017925
	500	0.014644	-0.01578	0.005586	0.009275
	750	0.012821	-0.01176	0.003683	0.005816
	1000	0.009643	-0.01178	0.002583	0.00422
	5000	0.003933	-0.00543	0.000496	0.000825
LSE	50	0.007252	-0.09039	0.061082	0.093738
	100	0.006455	-0.06402	0.037772	0.060589
	250	0.005879	-0.04108	0.016866	0.027737
	500	0.004612	-0.02729	0.00847	0.013762
	750	0.007582	-0.01753	0.005054	0.007517
	1000	0.005646	-0.0162	0.003569	0.005387
	5000	0.003076	-0.00635	0.000692	0.001039
WLSE	50	0.017581	-0.08063	0.058191	0.093202
	100	0.020565	-0.04859	0.033561	0.05424
	250	0.013928	-0.03219	0.014558	0.025039
	500	0.009952	-0.02117	0.006831	0.011352
	750	0.010665	-0.01402	0.004113	0.006301
	1000	0.007908	-0.0136	0.002897	0.00457
	5000	0.003604	-0.00577	0.000566	0.000896
ADE	50	0.03261	-0.06302	0.053849	0.084021
	100	0.025818	-0.04218	0.03154	0.049819
	250	0.016301	-0.02899	0.013158	0.021636
	500	0.009759	-0.02135	0.006652	0.011059
	750	0.009964	-0.01495	0.004284	0.00678
	1000	0.007658	-0.01392	0.002887	0.004579
	5000	0.003534	-0.00585	0.000565	0.000897
CvME	50	0.064212	-0.02921	0.067525	0.085902
	100	0.03813	-0.02914	0.038526	0.054513
	250	0.019487	-0.02571	0.016274	0.024633
	500	0.010943	-0.0203	0.008395	0.013062
	750	0.011476	-0.01337	0.005206	0.007583
	1000	0.008673	-0.01288	0.003585	0.005233
	5000	0.003662	-0.00571	0.000695	0.001029



**Table 6** Average bias and MSEs of the estimators for  $\alpha = 2$  and  $p = 0.7$

		Bias		MSE	
		$\hat{\alpha}$	$\hat{p}$	$\hat{\alpha}$	$\hat{p}$
MLE	50	0.07372	-0.042	0.110049	0.045603
	100	0.062605	-0.02372	0.059204	0.026281
	250	0.040866	-0.01311	0.023258	0.009907
	500	0.030569	-0.00893	0.011186	0.004779
	750	0.024302	-0.00819	0.007832	0.003313
	1000	0.021305	-0.00753	0.005433	0.002295
	5000	0.009233	-0.00375	0.001095	0.000477
	LSE	50	-0.03617	-0.10178	0.15932
100		0.011205	-0.05165	0.080768	0.038977
250		0.019934	-0.02423	0.029432	0.012814
500		0.020198	-0.0147	0.014256	0.006079
750		0.018246	-0.01178	0.010165	0.004278
1000		0.016654	-0.0102	0.006849	0.002847
5000		0.007945	-0.00446	0.001395	0.000588
WLSE		50	-0.00381	-0.08375	0.130536
	100	0.029262	-0.04207	0.068541	0.033551
	250	0.029727	-0.01877	0.024868	0.010882
	500	0.025742	-0.01147	0.011965	0.00509
	750	0.021797	-0.00962	0.008507	0.003564
	1000	0.018997	-0.00876	0.005789	0.002424
	5000	0.008589	-0.00408	0.001174	0.000503
	ADE	50	0.012258	-0.07409	0.120657
100		0.035621	-0.03733	0.06267	0.029554
250		0.029924	-0.01852	0.024325	0.010534
500		0.025172	-0.01175	0.011885	0.005086
750		0.021401	-0.00984	0.008462	0.003563
1000		0.018723	-0.0089	0.00577	0.002428
5000		0.008495	-0.00413	0.001173	0.000504
CvME		50	0.057488	-0.04411	0.156188
	100	0.056578	-0.02398	0.081187	0.034829
	250	0.036973	-0.01388	0.03028	0.012324
	500	0.028598	-0.00957	0.014595	0.0059
	750	0.023809	-0.00837	0.010365	0.004185
	1000	0.02081	-0.00765	0.00699	0.002789
	5000	0.008763	-0.00395	0.001408	0.000584

**Table 7** Average bias and MSEs of the estimators for  $\alpha = 3$  and  $p = 0.9$ 

		Bias		MSE	
		$\hat{\alpha}$	$\hat{p}$	$\hat{\alpha}$	$\hat{p}$
MLE	50	-0.00693	-0.07718	0.126464	0.024359
	100	0.032353	-0.03804	0.061012	0.010199
	250	0.041147	-0.01532	0.02726	0.004242
	500	0.036455	-0.00745	0.014003	0.00219
	750	0.03137	-0.0058	0.009701	0.001475
	1000	0.028266	-0.00499	0.007464	0.001119
	5000	0.011353	-0.00321	0.001492	0.000228
LSE	50	-0.10732	-0.11138	0.213604	0.052957
	100	-0.00812	-0.05099	0.09582	0.020827
	250	0.019089	-0.02381	0.03742	0.007553
	500	0.026372	-0.01129	0.019378	0.003868
	750	0.024707	-0.00876	0.013292	0.00254
	1000	0.024162	-0.00684	0.010145	0.001905
	5000	0.01084	-0.00359	0.002072	0.000392
WLSE	50	-0.07754	-0.10062	0.163501	0.038734
	100	0.006056	-0.04595	0.074239	0.014942
	250	0.029599	-0.01965	0.029987	0.005373
	500	0.031431	-0.00924	0.015549	0.002768
	750	0.028188	-0.00725	0.010735	0.001827
	1000	0.026388	-0.00586	0.008292	0.001384
	5000	0.011187	-0.00339	0.001668	0.000284
ADE	50	-0.07402	-0.09961	0.145472	0.034185
	100	0.00143	-0.04806	0.06676	0.013027
	250	0.026329	-0.02102	0.028818	0.005164
	500	0.029396	-0.01009	0.015153	0.002714
	750	0.026675	-0.00786	0.010553	0.001811
	1000	0.025357	-0.00629	0.008161	0.001371
	5000	0.010953	-0.00349	0.00166	0.000284
CvME	50	-0.00131	-0.06195	0.196431	0.040316
	100	0.041705	-0.02784	0.09697	0.01849
	250	0.038375	-0.01477	0.038486	0.007142
	500	0.035889	-0.0068	0.019953	0.003772
	750	0.03103	-0.00577	0.013637	0.00249
	1000	0.02889	-0.0046	0.010391	0.001876
	5000	0.011777	-0.00314	0.002093	0.000389

**Table 8** The list of the lifetime distribution to modelling COVID-19 patient data

$f_{TIR}(x) = \frac{2\alpha}{x^3} \exp\left(-\frac{\alpha}{x^2}\right) \left\{1 + \lambda - 2\lambda \exp\left(-\frac{\alpha}{x^2}\right)\right\},$	$\alpha > 0, \lambda \in [-1, 1]$
$f_{TR}(x) = \frac{x}{\alpha^2} \exp\left(-\frac{x^2}{2\alpha^2}\right) \left\{1 - \lambda + 2\lambda \exp\left(-\frac{x^2}{2\alpha^2}\right)\right\},$	$\alpha > 0, \lambda \in [-1, 1]$
$f_{TW}(x) = \frac{\alpha}{\beta} \left(\frac{x}{\beta}\right)^{\alpha-1} \exp\left(-\left(\frac{x}{\beta}\right)^\alpha\right) \left\{1 - \lambda + 2\lambda \exp\left(-\left(\frac{x}{\beta}\right)^\alpha\right)\right\},$	$\alpha, \beta > 0, \lambda \in [-1, 1]$
$f_{Weibull}(x) = \beta\alpha x^{\alpha-1} \exp(-\beta x^\alpha),$	$\alpha, \beta > 0$
$f_{Rayleigh}(x) = \frac{x}{\alpha^2} \exp\left(-\frac{x^2}{2\alpha^2}\right),$	$\alpha > 0$
$f_{TRTW}(x) = \beta\alpha x^{\alpha-1} \exp(-\beta x^\alpha) [1 + p(\beta x^\alpha - 1)],$	$\alpha, \beta > 0, p \in (0, 1)$

**Table 9** The MLEs and standard errors of parameters of the fitted distribution for dataset 1

	Parameter Estimates		
TLRTIR ( $\alpha, p$ )	249.5468 (67.3622)	0.4844 (0.3686)	
TIR ( $\alpha, \lambda$ )	91.8731 (19.3602)	-0.9113 (0.1886)	
IR ( $\alpha$ )	167.8621 (23.7392)		
TR ( $\alpha, \lambda$ )	18.5168 (2.1861)	0.7395 (0.2670)	
TW ( $\alpha, \beta, \lambda$ )	2.053352 (0.203708)	26.11543 (2.929975)	0.735174 (0.257507)
Weibull ( $\alpha, \beta$ )	1.87789 (0.18604)	20.85076 (1.669257)	
Rayleigh ( $\alpha$ )	15.0090 (1.0613)		
TRTW ( $\alpha, \beta, p$ )	1.866321 (0.097855)	0.003511 (0.000987)	0.012848 (0.180258)

**5.1 Dataset 1: COVID-19 patients data**

The first dataset consists of the time (in days) from the first positive to the first negative COVID-19 PCR test for 50 Israelis (more than 60 years and male). The recovery periods (days) were calculated from an anonymized dataset of recovered COVID-19 patients released to the public by the Israel Ministry of Health on November 25, 2020 [25]. The first dataset is as follows: 16, 16, 16, 14, 36, 9, 10, 11, 8, 9, 12, 10, 22, 5, 11, 17, 20, 12, 29, 12, 15, 25, 25, 24, 18, 13, 44, 14, 20, 19, 11, 10, 18, 21, 31, 9, 29, 12, 10, 10, 13, 12, 19, 33, 37, 16, 63, 9, 28, 16

The MLEs and standard errors (in parenthesis) of the parameters of the fitted distributions are presented in Table 9 and the comparison statistics are given for dataset 1 in Table 10. Also, Figure 3 provides the fitted cdfs and fitted pdfs for dataset 1.

**Table 10** The selection criterion statistics for dataset 1

	AIC	BIC	K-S	A*	W*	p-value
TLRTIR	355.81	359.634	<b>0.075421</b>	<b>0.373537</b>	<b>0.036377</b>	<b>0.938582</b>
TIR	355.7445	359.5685	0.082833	0.696839	0.089463	0.882608
IR	<b>354.0869</b>	<b>355.9989</b>	0.085887	0.605888	0.068869	0.854456
TW	366.4329	372.169	0.135886	1.18278	0.181822	0.314356
TR	364.5019	368.326	0.144622	1.188009	0.176251	0.246527
Weibull	367.4034	371.2274	0.146526	1.445075	0.229008	0.233298
Rayleigh	365.8247	367.7367	0.14654	1.575139	0.275655	0.233201
TRTW	369.4124	375.1484	0.148828	1.44123	0.226084	0.218029

Bold indicates the best model according to the criteria in the relevant column

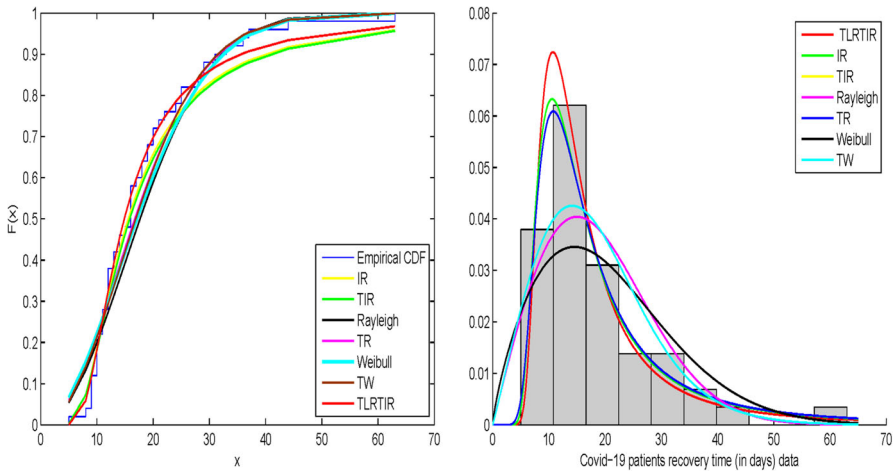


**Fig. 3** Fitted cdfs (left panel) and fitted pdfs (right panel) for dataset 1

As a result of the analysis of dataset 1, it is observed that the best fitted model is TLRTIR ( $\alpha, p$ ) according to  $A^*, W^*, K-S$  and its p-value. By assuming the recovery times distribute TLRTIR ( $\alpha = 249.5468, p = 0.4844$ ) distribution, we estimate the probabilities of recovery times of COVID-19 patients more than 60 years old and male. In this regard, estimated probabilities according to recovery times are given in Table 11.

From Table 11, the probability of recovery of a COVID-19 patient (more than 60 years old and male) within the first two weeks after contracting the virus is approximately 45%. The probability of recovery in patients having to the same characteristics within the first three weeks is approximately 72%. It can be concluded that in the first 8 weeks after infection, about 95% of the patients recovered. The expected value of TIRTIR ( $\alpha = 249.5468, p = 0.4844$ ) distribution is approximately 21. This means the recovery time of the COVID-19 patient (more than 60 years and male) is about 21 days.

**Table 11** Estimated probabilities of the recovery times of COVID-19 patients for dataset 1

Recovery time	Estimated probability	Recovery time	Estimated probability
<7 days	0.0212	<4 weeks	0.8395
<8 days	0.0585	<5 weeks	0.8961
<9 days	0.1144	<6 weeks	0.9275
<10 days	0.1821	<7 weeks	0.9466
<11 days	0.2541	<8 weeks	0.9591
<12 days	0.3251	<9 weeks	0.9676
<13 days	0.3917	<10 weeks	0.9737
<14 days	0.4525	<11 weeks	0.9783
<15 days	0.507	<12 weeks	0.9817
<16 days	0.5554	<13 weeks	0.9844
<17 days	0.598	<14 weeks	0.9866
<18 days	0.6356	<15 weeks	0.9883
<19 days	0.6686	<16 weeks	0.9897
<20 days	0.6978	<17 weeks	0.9909
<21 days	0.7235	<18 weeks	0.9918

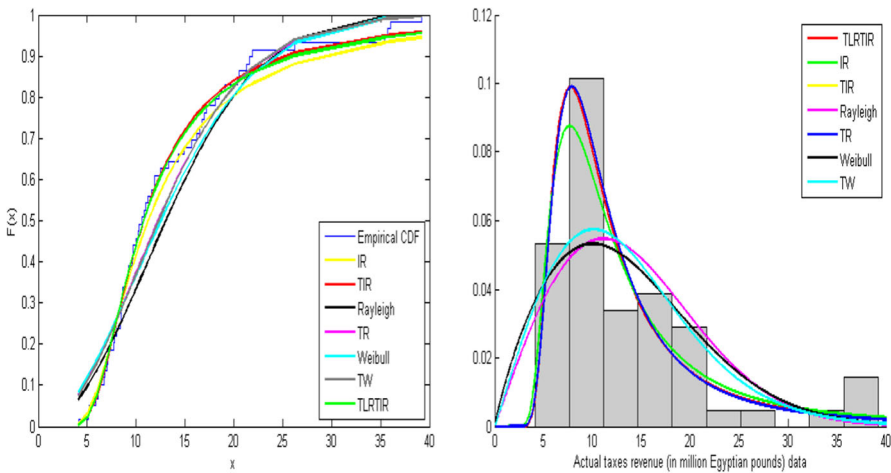
**Table 12** The MLEs of parameters of the fitted distribution for dataset 2

	Parameter Estimates		
TLRTIR ( $\alpha, p$ )	127.2051 (29.9773)	0.4521 (0.3109)	
TIR ( $\alpha, \lambda$ )	105.5277 (19.4813)	0.4040 (0.3522)	
IR ( $\alpha$ )	87.6003 (11.4045)		
TR ( $\alpha, \lambda$ )	13.1314 (1.3328)	0.6423 (0.6423)	
TW ( $\alpha, \beta, \lambda$ )	2.0182 (0.1875)	18.5726 (1.8412)	0.6431 (0.2339)
Weibull ( $\alpha, \beta$ )	1.8403 (0.1711)	15.3060 (1.1512)	
Rayleigh ( $\alpha$ )	11.0828 (0.7214)		
TRTW ( $\alpha, \beta, p$ )	1.8414 (0.1343)	0.0066 (0.0027)	0.0041 (0.1848)

**Table 13** The selection criterion statistics for dataset 2

	AIC	BIC	K-S	A*	W*	p-value
TLRTIR	382.5586	386.7137	<b>0.0619</b>	0.2741	0.0333	<b>0.9775</b>
TIR	382.2614	386.4165	0.0655	<b>0.2553</b>	<b>0.0329</b>	0.9621
IR	<b>381.1754</b>	<b>383.2529</b>	0.0822	0.4637	0.0635	0.8203
TR	395.4216	399.5766	0.1299	1.4934	0.2173	0.2720
TW	397.4121	403.6447	0.1325	1.5029	0.2213	0.2515
Weibull	398.5811	402.7361	0.1432	1.8404	0.2804	0.1780
Rayleigh	397.4217	399.4992	0.1721	2.2104	0.3773	0.0608
TRTW	400.5824	406.8150	0.1421	1.8286	0.2765	0.1842

Bold indicates the best model according to the criteria in the relevant column

**Fig. 4** Fitted cdfs (left panel) and fitted pdfs (right panel) for dataset 2

## 5.2 Dataset 2: Actual taxes revenue data

The second dataset is obtained by [26]. The data includes of the monthly actual taxes revenue (in million Egyptian pounds) in Egypt from January 2006 to November 2010. The second dataset are as follows: 5.9, 20.4, 14.9, 16.2, 17.2, 7.8, 6.1, 9.2, 10.2, 9.6, 13.3, 8.5, 21.6, 18.5, 5.1, 6.7, 17, 8.6, 9.7, 39.2, 35.7, 15.7, 9.7, 10, 4.1, 36, 8.5, 8, 9.2, 26.2, 21.9, 16.7, 21.3, 35.4, 14.3, 8.5, 10.6, 19.1, 20.5, 7.1, 7.7, 18.1, 16.5, 11.9, 7.8, 6, 12.5, 10.3, 11.2, 6.1, 8.4, 11, 11.6, 11.9, 5.2, 6.8, 8.9, 7.1, 10.8.

For the second dataset, the MLEs and standard errors (in parenthesis) of the parameters of the fitted distributions are given in Table 12, and the selection criteria statistics are presented in Table 13. Also, Figure 4 illustrates the fitted cdfs and fitted pdfs for dataset 2. For two datasets, some plots such as Kernel densities, Probability-Probability (P-P) and Quantile-Quantile (Q-Q) plots are respectively given in Figs. 5-7.

From Figures 5-7, we can easily see that there are good fits between TLRTIR ( $\alpha, p$ ) distribution and datasets 1-2. Also, it is observed that the TLRTIR ( $\alpha, p$ ) distribution

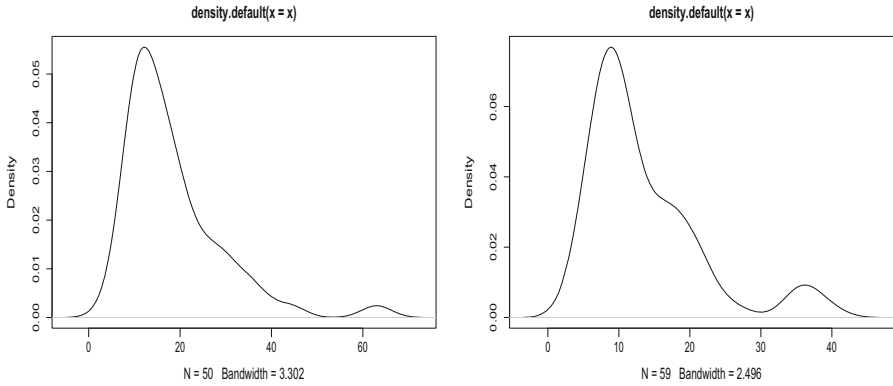


Fig. 5 Kernel density for dataset 1 (left panel) Kernel density for dataset 2 (right panel)

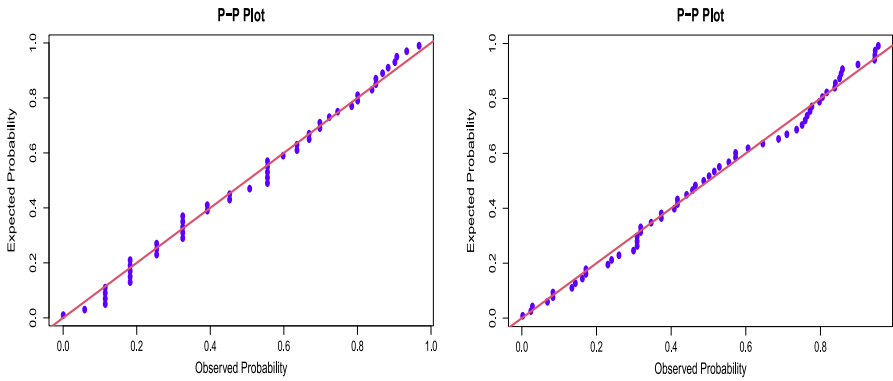


Fig. 6 P-P plot for dataset 1 (left panel) P-P plot for dataset 2 (right panel)

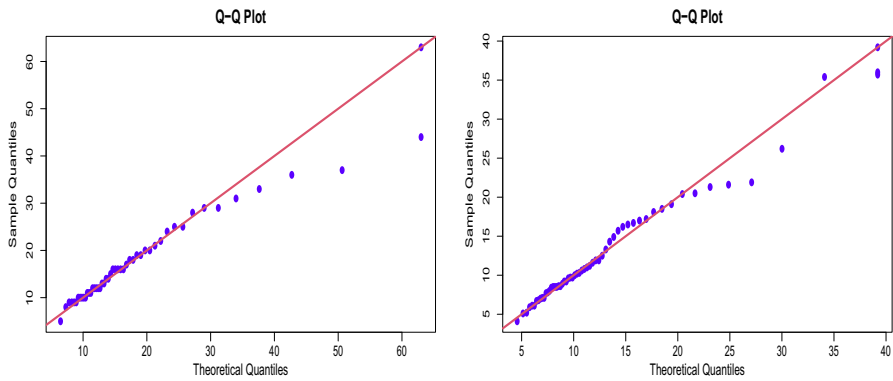


Fig. 7 Q-Q plot for dataset 1 (left panel) Q-Q plot for dataset 2 (right panel)

is the best fit to the datasets in Figs. 3-4. So Figures 3-7 support the results in Table 10 and Table 13.

## 6 Conclusion

In this study, we suggest a new lifetime distribution which is useful in modelling medical science data. We obtain five estimators such as MLE, LSE, WLSE, ADE, and CvME of the unknown parameters of the TLRTIR  $(\alpha, p)$  distribution. A comprehensive Monte Carlo simulation study is considered to assess the performances of these estimators via biases and MSEs. As a result of the simulation study, we observe that as the sample sizes increase the MSEs and biases of all estimators decrease for all parameter values as expected. We recommend the maximum likelihood and Anderson-Darling method for point estimation of  $\alpha$  and  $p$ . Two real data applications are performed to show the usefulness of TLRTIR  $(\alpha, p)$  distribution. In real data illustration, we provide the data sets regarding the recovery time (in days) of COVID-19 patients. The results of real data applications show that the best fitted model is TLRTIR  $(\alpha, p)$  according to K-S, its p-value,  $A^*$ , and  $W^*$  for data set 1 while the best fitted model is TLRTIR  $(\alpha, p)$  according to all selection criteria for data set 2.

In previous studies, Barman et al. [27] emphasized that the probability of recovery period of a COVID-19 patient within 20 days is about 43%. Sutiningsih et al. [28] reported that the mean recovery time in COVID-19 patients is 20.63 days. Moreover, Voinsky et al. [29] found that the average recovery time in COVID-19 patients is approximately 15 days. Our results support previous studies. We observe that the estimated mean recovery time is found about 21 days for dataset 1. On the other hand, we estimate that the probability of recovery period of a COVID-19 patient within two weeks is about 45%.

In conclusion, we provide a new perspective on the interpretation and statistical evaluation of clinical data on COVID-19 patients. We also have shown that a new lifetime distribution is not only included in statistical theory and that they have the potential to be used in interpreting the COVID-19 data. To our knowledge, this is the first study providing the estimated probabilities of the recovery time in COVID-19 patients using a lifetime distribution. One of the advantages of this study is that the calculated estimates in the real data analysis section are similar to the previous studies. In future times, extensive research should be conducted on the recovery periods of COVID-19 patients.

**Acknowledgements** The author is thankful to the Israel Ministry of Health for providing public access to anonymized Covid-19 patient records and to Prof. Dr. David Gurwitz for his help in obtaining data of Covid-19 patients. The author sincere thanks to two anonymous reviewers for their helpful comments.

## References

1. Shaw, W.T., Buckley, I.R.: The alchemy of probability distributions: beyond Gram-Charlier expansions, and a skew-kurtotic-normal distribution from a rank transmutation map. arXiv preprint [arXiv:0901.0434](https://arxiv.org/abs/0901.0434) (2009)
2. Aryal, G., Tsokos, C.P.: Transmuted Weibull distribution: a generalization of the Weibull probability distribution. Eur. J. Pure Appl. Math. **4**(2), 89–102 (2011)
3. Merovci, F.: Transmuted lindley distribution. Int. J. Open Problems Compt. Math **6**, 63–72 (2013)



4. Merovci, F.: Transmuted rayleigh distribution. *Austrian J. statistics* **42**, 21–31 (2013)
5. Ahmad, A., Ahmad, S.P., Ahmed, A.: Transmuted inverse Rayleigh distribution: a generalization of the inverse Rayleigh distribution. *Math. Theory and Model.* **4**, 90–98 (2014)
6. Haq, M.A.: Transmuted exponentiated inverse Rayleigh distribution. *J. Stat. Appl. Prob* **5**, 337–343 (2016)
7. Cordeiro, G.M., Saboor, A., Khan, M.N., Provost, S.B., Ortega, E.M.: The transmuted generalized modified Weibull distribution. *Filomat* **31**, 1395–1412 (2017)
8. Tanış, C., Saraçoğlu, B., Kuş, C., Pekgor, A.: Transmuted complementary exponential power distribution: properties and applications. *Cumhuriyet Sci. J.* **41**(2), 419–432 (2020)
9. Saraçoğlu, B., Tanış, C.: A new lifetime distribution: transmuted exponential power distribution. *Commun. Faculty of Sci. Univ. Ankara Series A1 Math. Statistics* **70**(1), 1–14 (2021)
10. Alizadeh, M., Merovci, F., Hamedani, G.G.: Generalized transmuted family of distributions: properties and applications. *Hacet J Math Stat* **46**, 645–667 (2017)
11. Granzotto, D.C.T., Louzada, F., Balakrishnan, N.: Cubic rank transmuted distributions: inferential issues and applications. *J. Stat. Comput. Simul.* **87**, 2760–2778 (2017)
12. Saraçoğlu, B., Tanış, C.: A new statistical distribution: cubic rank transmuted Kumaraswamy distribution and its properties. *J. Natl. Sci. Found.* **46**(4), 505–518 (2018)
13. Ogunde, A.A., Chukwu, A.U., Agwuegbo, S.O.: The characterization of the cubic rank inverse Weibull distribution. *Asian Res. J. Math.* **16**(7), 20–33 (2020)
14. Bhatti, F.A., Hamedani, G.G., Najibi, S.M., Ahmad, M.: Cubic rank transmuted modified burr III distribution: development, properties, characterizations and applications. *J. Data Sci.* **18**(1), 303–323 (2020)
15. Bhatti, F.A., Hamedani, G.G., Sheng, W., Ahmad, M.: Cubic rank transmuted modified burr III pareto distribution: development, properties, characterizations and applications. *Int. J. Statistics and Prob.* **35**, 105–116 (2019)
16. Sakthivel, K.M., Rajitha, C.S., Dhivakar, K.: Two parameter cubic rank transmutation of Lindley distribution. In: *AIP Conference Proceedings*, AIP Publishing LLC **2261**(1), 030086 (2020)
17. Aslam, M., Hussain, Z., Aşghar, Z.: Cubic transmuted-G family of distributions and its properties. *Stochastics and Quality Control* **33**(2), 103–112 (2018)
18. Balakrishnan, N., He, M.: A record-based transmuted model, *Advance Online Publication* (2021)
19. Tanış, C., Saraçoğlu, B.: On the record-based transmuted model of Balakrishnan and He based on weibull distribution, *Communications in Statistics-Simulation and Computation*, <https://doi.org/10.1080/03610918.2020.1740261> (2020)
20. Tanış, C., Saraçoğlu, B., Kuş, C., Pekgor, A., Karakaya, K.: Transmuted Lower Record Type Fréchet Distribution with Lifetime Regression Analysis Based on Type I-Censored Data. *Journal of Statistical Theory and Applications* (2021). <https://doi.org/10.2991/jsta.d.210115.001>
21. Rényi, A.: On measures of entropy and information. In: *Proceedings of the 4th Fourth Berkeley Symposium on Mathematical Statistics and Probability*, University of California Press, Berkeley (1961)
22. Gradshteyn, I.S., Ryzhik, I.M.: *Table of Integrals, Series, and Products*. Academic press, US (2014)
23. Shaked, M., Shanthikumar, J.G.: *Stochastic Orders and their Applications*. Academic Press, London (1994)
24. Fletcher, R.: *Practical Methods of Optimization*. John and Sons, Chichester
25. <https://data.gov.il/dataset/Covid-19>, Accessed 25 Nov 2020
26. Almarashi, A.M., Badr, M.M., Elgarhy, M., Jamal, F., Chesneau, C.: Statistical inference of the half-logistic inverse Rayleigh distribution. *Entropy* **22**(4), 449 (2020). <https://doi.org/10.3390/e22040449>
27. Barman, M.P., Rahman, T., Bora, K., Borgohain, C.: COVID-19 pandemic and its recovery time of patients in India: a pilot study. *Diabetes & Metabolic Syndrome: Clin Res & Rev* **14**(5), 1205–1211 (2020)
28. Sutningsih, D., Rahatina, V.E.F., Saraswati, L.D., Prabowo, Y., Sugiharto, A., Wibowo, M.A. Clinical Symptoms, Comorbidities, and Recovery Period for Covid-19 Patients in Central Java Province, Indonesia, *Annals of Tropical Medicine & Public Health*, **24**(1), (2021). <https://doi.org/10.36295/ASRO.2021.24119>
29. Voinsky, I., Baristaite, G., Gurwitz, D.: Effects of age and sex on recovery from COVID-19: Analysis of 5769 Israeli patients. *J. Infect.* **81**(2), e102–e103 (2020). <https://doi.org/10.1016/j.jinf.2020.05.026>

**Publisher's Note** Springer Nature remains neutral with regard to jurisdictional claims in published maps and institutional affiliations.

Springer Nature or its licensor holds exclusive rights to this article under a publishing agreement with the author(s) or other rightsholder(s); author self-archiving of the accepted manuscript version of this article is solely governed by the terms of such publishing agreement and applicable law.